Nanoscale

Dynamic Article Links

Cite this: *Nanoscale*, 2012, **4**, 2720

www.rsc.org/nanoscale

PAPER

In vivo studies on angiogenic activity of two designer self-assembling peptide scaffold hydrogels in the chicken embryo chorioallantoic membrane

Xi Liu,[a] Xiumei Wang,*[a] Akihiro Horii,[b] Xiujuan Wang,[c] Lin Qiao,[a] Shuguang Zhang[d] and Fu-Zhai Cui[a]

Received 1st January 2012, Accepted 1st March 2012
DOI: 10.1039/c2nr00001f

The rapid promotion of angiogenesis is critical for tissue engineering and regenerative medicine. The angiogenic activity of tissue-engineered scaffolds has already been the major criterion for choosing and designing ideal biological materials. We here report systematic *in vivo* studies on the angiogenic activity of two functionalized self-assembling peptides PRG (Ac-$(RADA)_4$GPRGDSGYRGDS-$CONH_2$) and KLT (Ac-$(RADA)_4G_4$KLTWQELYQLKYKGI-$CONH_2$) using the chicken embryo chorioallantoic membrane (CAM) assay. 3D migration/sprouting bead assays showed that the two functional motifs PRGDSGYRGDS and KLTWQELYQLKYKGI improved the bioactivities of the self-assembling peptide RADA16-I (Ac-$(RADA)_4$-$CONH_2$) dramatically and provided ideal synthetic microenvironments for endothelial cell migration and cordlike structure sprout formation. A CAM assay was carried out to assess the efficiency of various peptide scaffolds in inducing capillary invasion *in vivo*. Among these three peptide scaffolds, the functionalized peptide scaffold RAD/KLT presented a significantly better angiogenic activity inducing CAM tissue invasion and new capillary vessel formation within the scaffolds in the absence of VEGF. With the addition of VEGF, more newly formed vessel lumen could be observed in all peptide scaffolds. Our results suggested that the functionalized peptide scaffolds had satisfactory angiogenic properties, and may also have wide potential applications in tissue regeneration.

Introduction

Vascular network reconstruction within tissue engineered substitutes remains the major challenge so far for tissue engineering and regenerative medicine, which is vitally important in determining the clinical success of transplantation and new tissue regeneration.[1–3] As we all know, oxygen and nutrients required for cell survival are limited to a distance of approximately 200–400 μm from the supplying blood vessel, thus it means transplanted cells or invasive endogenous cells in the centre of engineered constructs will undergo apoptosis if a blood supply cannot be established in a short time.[4,5] Therefore, the promotion of angiogenesis within transplanted tissue engineered scaffolds and newly grown tissue is extremely important for almost all types of tissue regeneration and tissue engineering.

Angiogenesis refers to the fundamental process of new capillary formation from pre-existing blood vessels, which consists of several consecutive steps that include 1) the stimulation of endothelial cells (ECs) by growth factors; 2) the subsequent degradation of the extracellular matrix (ECM) by proteolytic enzymes; 3) proliferation, migration, and invasion of ECs in the ECM forming new capillary tubes; and finally 4) the recruitment of smooth muscle cells and pericytes stabilizing the newly formed capillary network.[6,7] Therefore, the regulation of endothelial cell survival and migration is essential for angiogenesis, which is strongly dependent on the interaction of ECs with ECM proteins *via* cell adhesion molecules, and the activities of growth factors and cytokines. In the absence of either, endothelial cells rapidly undergo apoptosis.

These natural EC niches provide important cues for designing the material parameters of tissue-engineered scaffolds. Several types of biomaterials including collagen, fibrin, alginate gels, and PLGA have been used as tissue-engineered scaffold for angiogenesis studies.[8–15] However, in most systems, high concentrations of soluble angiogenic growth factors are required for cell survival and effective vascular system formation. Although these angiogenic cytokines or growth factors present remarkable efficacies in promoting new vascular formation, their usage should be limited in constructing certain tissue engineered scaffolds because of some imperative processes required for the scaffolds, such as thermal processing and sterilization, and the high risks of hyper-stimulation and other unwanted effects arising *in vivo*.[16] These problems

[a]*State Key Laboratory of New Ceramics and Fine Processing, Department of Materials Science and Engineering, Tsinghua University, Beijing 100084, China. E-mail: wxm@mail.tsinghua.edu.cn; Fax: +86-10-62771160; Tel: +86-10-62782966*
[b]*Olympus America Inc., 3500 Corporate Parkway, Center Valley, PA 18034, USA*
[c]*Jilin Hepatology Hospital, Changchun 130061, China*
[d]*Center for Biomedical Engineering, Massachusetts Institute of Technology, 77 Massachusetts Avenue, Cambridge, MA 02139, USA*

could probably be overcome in part by conjugating bioactive short peptide motifs with self-assembling RADA16-I (Ac-$(RADA)_4$-$CONH_2$) peptide nanofiber scaffolds to maintain the bioactivity and biosafety at the same time. Moreover, the fiber diameter of the peptide scaffolds is around 15–20 nm which is significantly smaller than that of endothelial cells (~5–10 μm), thus the endothelial cells can be fully surrounded by the scaffolds, much like the extracellular environment *in vivo*.[17]

We previously reported an *in vitro* study of the angiogenic activities of two designer self-assembling peptide nanofiber scaffolds RAD/PRG and RAD/KLT. The functional motif PRG (PRGDSGYRGDS) is a 2-unit RGD binding peptide with two similar RGD binding sequences PRGDS and YRGDS, which has been proven to increase cell adhesion and proliferation remarkably.[18] The functional motif KLT (KLTWQELYQLKYKGI) is a VEGF (vascular endothelial growth factor)-mimicking peptide, which could activate the VEGF-dependent signaling pathway as a VEGF agonist.[19] These two functionalized peptide scaffolds have been proven to have distinct bioactivities to promote human umbilical vein endothelial cell (HUVEC) survival, proliferation, migration, and morphological differentiation *in vitro*.[20] In the present study, we therefore report the evaluations of the *in vivo* angiogenic activities of these two functionalized peptide scaffold hydrogels RAD/PRG and RAD/KLT using the chick embryo chorioallantoic membrane (CAM) assay.

The chick embryo CAM is an extra-embryonic membrane lining the inner shell membrane, which is formed by the fusion of the ectodermal epithelium (chorion) and the endodermal epithelium (allantois) from incubation day 4 with scattered undifferentiated blood vessels in the mesoderm. Until incubation day 8, these primitive vessels grow rapidly and differentiate into a capillary network beneath the ectoderm that serves as a transient gas exchange surface with the outer environment. The chick embryo CAM has therefore been used as an *in vivo* model for the evaluation of angiogenesis because of its extensive vascularization. The CAM assay is probably the most extensively used method for assaying angiogenesis *in vivo* due to its superior advantages over other animal models.[21,22] First, the CAM assay is relatively easy and inexpensive, and thus quite suitable for large-scale screening. Second, the CAM consists of a thin, planar vascular network membrane, which is well adapted for direct observation using stereo-microscopy. Moreover, the CAM provides an easily accessible neovascular network in transparent matrix, which allows direct visualization and quantification of blood vessels before and after scaffold implantation.

In this study, the functionalized self-assembling peptide scaffold hydrogels RAD/PRG and RAD/KLT with or without VEGF were transplanted onto the chick embryo CAM to assay their angiogenic activities. These two designer functionalized peptide scaffold hydrogels not only significantly promote endothelial cell migration and sprouting *in vitro*, but also induce abundant capillary vessel lumen *in vivo*.

Materials and methods

Peptide solution preparation and gel formation

The bioactive motifs PRG and KLT were used to functionalize the self-assembling peptide RADA16-I by direct extension from its C-terminal forming functionalized self-assembling peptides PRG (Ac-$(RADA)_4$GPRGDSGYRGDS-$CONH_2$) and KLT (Ac-$(RADA)_4G_4$KLTWQELYQLKYKGI-$CONH_2$). These self-assembling peptides were custom-synthesized through solid phase synthesis by CPC Scientific (Purity >80%, San Jose, CA) and dissolved in water at a concentration of 1% (10 mg ml^{-1}, w/v) with 30-minute sonication. All peptide solutions were filter-sterilized by 0.22 μm syringe filter for subsequent use.

The functionalized peptide solutions were mixed with RADA16-I solution in a volume ratio of 1 : 1 to have a functionalized peptide mix (RAD/PRG or RAD/KLT). Fig. 1 shows the molecular models of the designer peptides and schematic illustrations of the self-assembling peptide nanofiber scaffold hydrogels. The functionalized peptide mix underwent self-assembly forming a uniform and interweaved long nanofiber structure with extrusion of functional motifs from the nanofiber backbone. The self-assembling peptide solutions convert to hydrogels by adding PBS or cell culture medium or adjusting the pH value to neutral.[17] The microstructures of the peptides hydrogel were examined by scanning electron microscopy (SEM) and atomic force microscopy (AFM) (Fig. 1).

Transwell inserts (Millipore, MA) were used for peptide gel formation as previously reported. Briefly, the inserts were placed in a 24-well culture plate with 400 μl of culture medium in each well. Then 100 μl of peptide solution was loaded directly into the inserts, 400 μl of culture medium was carefully added onto the hydrogel and finally they were incubated overnight at 37 °C. The medium was changed twice or more to equilibrate the hydrogel to physiological pH prior to use.

3D migration/sprouting bead assay

Primary isolated HUVECs were commercially obtained from Lonza Inc. (Walkersville, MD) and routinely grown in endothelial growth media EGM-2 (Lonza Inc., Walkersville, MD) on regular tissue-culture plates. All the experiments were conducted with cells between passage 5 and passage 8. HUVECs were mixed with dextran-coated Cytodex microcarrier beads (sigma) at a concentration of 400 cells per bead in 1 ml of EGM-2 medium. Beads with cells were shaken gently every 20 min for 4 h at 37 °C and 5% CO_2 to form a monolayer cell culture on the surfaces of the beads. After another 12–16 h cell culture, beads with cells were embedded at a concentration of 1200 cell-coated beads ml^{-1} in different types of hydrogels, RADA16-I, RAD/PRG, RAD/KLT, collagen type-I, and Matrigel with or without VEGF (20 ng ml^{-1}). Collagen type-I and Matrigel were used as positive controls. The bead assays were monitored for 3 days to characterize the different cell response behaviors to different hydrogel environments. To distinguish the migration and proliferation cells, the results of the 4 h, 12 h, 1 day, 2 day and 3 day cultures were evaluated. Cells were stained with Rhodaminphalloidin and SYTOX®Green (Invitrogen) for labeling F-actin and nuclei, respectively. Images were taken using a phase contrast microscope and laser confocal scanning microscope (LSM, Leica SP5).

The number and length of sprouts from the peptide scaffold were quantified as previously reported.[23] Briefly, high-resolution images of beads were captured on a Zeiss Axio Observer microscope with a 10× objective. Images were then analyzed in NIH ImageJ. The number of sprouts per beads was determined,

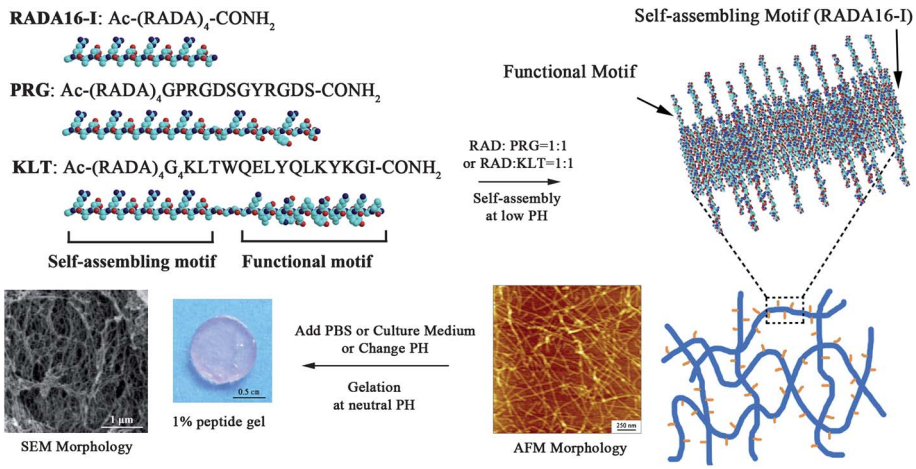

Fig. 1 Molecular models of designer peptides and schematic illustrations of self-assembling peptide nanofiber scaffolds. Hydrophobic alanine side groups are present on one side of the self-assembling motif RADA16-I β-sheet and the other side is populated with alternating positive and negative charges due to the arginine and aspartic acid residues, respectively. The functional motifs extrude from the nanofiber backbone. The typical AFM morphology of the self-assembling functionalized peptide solutions and SEM morphology of the functionalized peptide nanofiber scaffold gel are also presented.

and the sprout length was measured in arbitrary units. At least 25 beads were assessed for each group.

In vivo chick embryo CAM assay

Fertilized specific pathogen-free (SPF) chicken eggs were received from Charles River Laboratories (Boston, USA) at incubation day 0 and then incubated at 37 °C with approximately 60–65% humidity after cleaning with 70% ethanol. On incubation day 3, 2–3 ml of albumen was aspirated with a syringe needle so as to detach the developing CAM from the top part of the shell. On day 6, a window of around 1.5 cm^2 was gently opened with a scalpel on the wide end of the egg without damaging the embryo. The window was then sealed with transparent tape to prevent dehydration and possible infections before returning to the hatching incubator. On day 8, sterilized test hydrogel alone/or containing 20 ng VEGF was placed directly on the top of the CAM by peeling off the inner shell membrane. Collagen type-I gel and Matrigel were tested as controls. Fig. 2 shows a schematic illustration of the *in vivo* CAM study.

The SPF eggs were checked every day and the dead ones removed in time. There were 20 SPF survival eggs for each experimental group. On day 12, the covering tapes were removed and the test materials examined with the surrounding CAMs through the windows under a stereo-microscope, with digitized images taken at 8× using a Nikon dissecting microscope. A 0.5 × 0.5 cm^2 grid was then added to the digital CAM images. The vascular density in the hydrogels was expressed as the percentage of the squares in the mesh which contained blood vessels.[24] Then, the CAMs with test hydrogels were collected and fixed in 10% formalin, embedded in paraffin, sectioned, and finally stained with hematoxylin-eosin (H&E) for standard histopathological evaluation after 4 days of implantation.

Statistical methods

A total of 25 and 10 readings were carried on sprout quantification *in vitro* and the vessel density test *in vivo*, respectively. Data were analyzed by t-test. The values were considered significantly different at $P < 0.01$.

Results

Endothelial cell migration and sprouting are the most important steps in angiogenesis. The functionalized peptide scaffold hydrogels RAD/PRG and RAD/KLT have been shown to significantly enhance endothelial cell survival, attachment, proliferation, migration, and morphological differentiation compared with the pure RADA16-I scaffold hydrogel. In this study, we therefore examined whether HUVECs growing on dextran-coated beads in test scaffold hydrogels would respond to the different cell niche and migrate or sprout from the beads into the materials.

To make sure the migration cells were distinguished from proliferation cells, the one-day cell culture was chosen to reflect the preferences of endothelial cell migration in response to the microenvironments of the surrounding scaffold hydrogels from

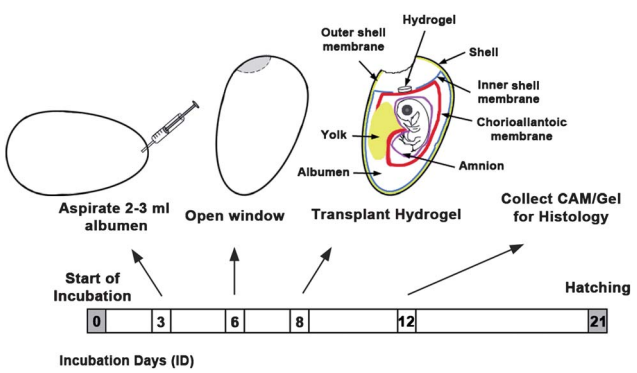

Fig. 2 Schematic illustration of the *in vivo* CAM procedure. Remove 2–3 ml of albumen from 3 day-old embryonated eggs with a syringe needle, then open a window on day 6 of incubation. On day 8, place hydrogel on the chorioallantoic membrane and collect CAM and gel for further evaluation 4 days post implantation.

the dextran-coated beads in the absence of VEGF (Fig. 3 and Table 1). The typical morphology of endothelial cell-coated Cytodex microcarrier beads with a diameter of around 200 μm is shown in Fig. 3a. As a positive control, the endothelial cells preferred to migrate away extensively from the beads to surrounding collagen gel without forming sprouts (Fig. 3b). Quite similar cell behavior occurred in the RAD/PRG and RAD/KLT groups, as shown in Fig. 3e and 3f, which indicated that the functional motifs PRG and KLT successfully presented in a manner of bioactive ligands of synthetic peptide materials and modulated EC migration mimicking the natural extracellular matrix. Visibly less cell migration occurred to the RADA16-I scaffold (Fig. 3d) which also confirmed the functions of PRG and KLT in the peptide scaffold hydrogels, in agreement with the results we previously reported.[20] Due to lots of growth factors in Matrigel, the endothelial cells underwent morphological differentiation with little cell migration. It should be noted that no sprouting was observed in the absence of VEGF in all peptide hydrogels and collagen gel.

In order to avoid subjective bias and interference from neighboring beads, at least 10 isolated beads without neighbors within a radius of 500 μm for each type of hydrogel were selected for cell counting to quantitatively characterize cell migration from the central bead. The result showed that the number of cells migrating to RAD/PRG or RAD/KLT was about twice as many as to the RADA16-I scaffold, which was similar to the cell number migrating to the collagen sample, as shown in Table 1. This quantitative result was in accordance with the morphology result mentioned above.

Fig. 4 shows that the HUVECs migrated, proliferated, and formed well-defined sprouts with hollow lumens from the dextran beads in the presence of VEGF (20 ng ml^{-1}) in the self-assembling peptide scaffold hydrogels after 2 days of cell culture. The first sprouts had apparently appeared with short, tiny cordlike structures within one day (data not shown). Then, the newly formed sprouts continued to extend from the beads with increasing sprouting numbers, length, and branches over time, as shown in Fig. 4a–c. Although sprout formations were observed in all peptide hydrogels, the HUVECs in the RAD/PRG and RAD/KLT gels produced much longer cellular processes and more branches compared with those in the RADA16-I gel (Fig. 5), which indicated that the functional motifs PRG and KLT might have promising effects on cell growth and increase the responsivity of endothelial cells to VEGF for sprouting. RAD/KLT supports the highest sprout formation and average sprout length as shown in Fig. 5. For the collagen gel control, a fluorescence stain was used to label the HUVEC-coated beads because of the non-transparence and coarse gel texture under phase contrast microscope. Sprouting could also be identified in the collagen gel, while the numbers of sprouting and branching structures were much lower than those in the functionalized self-assembling peptide hydrogels (Fig. 4d).

Since the functionalized self-assembling peptide scaffold hydrogels RAD/PRG and RAD/KLT have been shown to have distinct capabilities to promote endothelial cell migration and sprouting *in vitro*, we then examined their *in vivo* angiogenic activities with or without VEGF in the CAM assay.

The gross evaluations and morphologies of CAM tissue responses to various scaffolds in the absence of VEGF are shown in Fig. 6. Four days after deposition of the hydrogels on top of the CAM, the hydrogels were incorporated with the CAM quite well, as shown in Fig. 6A1–E1. In addition, a quantitative vascular density assay showed that RAD/PRG and RAD/KLT resulted in more intense angiogenesis than RADA 16-I (Table 2). Representative photomicrographs of H&E stained histological sections are presented at low magnification (Fig. 6A2–E2) and high magnification (Fig. 6A3–E3), respectively. Neutrophils and monocytes were not obvious at the interface between the gels and

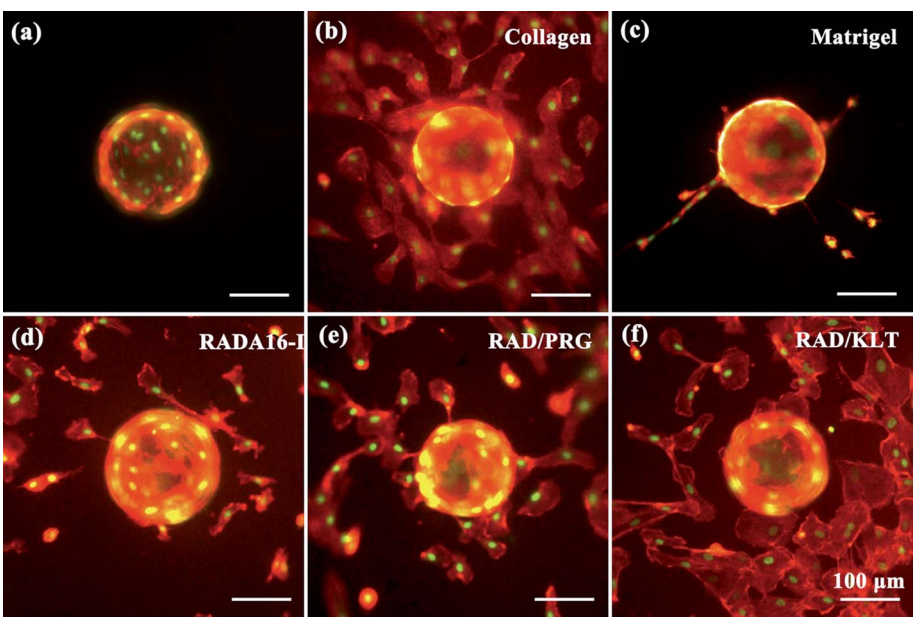

Fig. 3 HUVEC migration to different surrounding scaffold hydrogels after 1 day culture in the absence of VEGF. a, cells plated uniformly on the beads. Cells migration from beads to: b, collagen type-I gel; c, Matrigel; d, RADA16-I; e, RAD/PRG; f, RAD/KLT. The scale bar represents 100 μm for all panels. Red is for F-actin and green is for nuclei.

Table 1 The numbers of endothelial cells migrated from beads to different surrounding scaffold hydrogels

Scaffolds	Collagen type-I	Matrigel	RADA16-I	RAD/PRG	RAD/KLT
Cell no.[a]	37.9 ± 3.9[b]	7.4 ± 2.6	19.9 ± 2.2	34.9 ± 3.4[b]	32.5 ± 4.9[b]

[a] Data are presented as mean ± SD; $n = 10$. [b] $p < 0.01$ *vs.* Matrigel and RADA16-I, t-test.

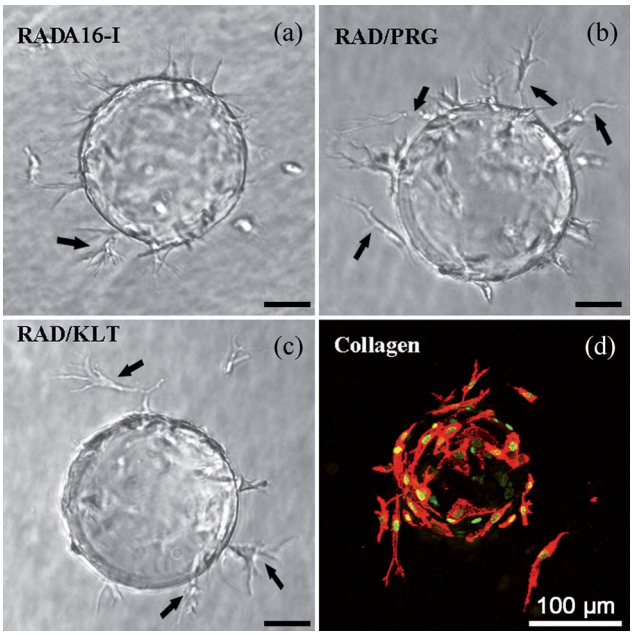

Fig. 4 HUVECs form EC-tube like sprouts from peptide scaffold hydrogels of RADA16-I, RAD/PRG and RAD/KLT after 2 days of culture. Collagen type-I gel was used as a positive control. Red is for F-actin and green is for nuclei. Black arrows indicate the cordlike structures sprouting from the peptides.

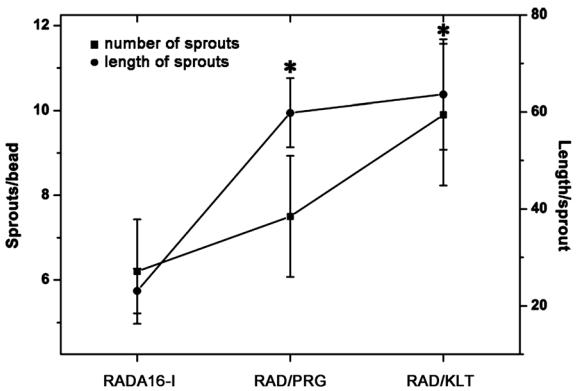

Fig. 5 Quantification of sprouts from peptide scaffold hydrogels of RADA16-I, RAD/PRG and RAD/KLT after 2 days of culture ($n = 25$). *$p < 0.01$ *vs.* length of sprout from RADA16-I.

local tissue indicating that no severe inflammatory response was induced by any of the implanted scaffolds. Hyperplasia of the CAM tissues under the implanting scaffolds was clearly observed in all cases. Epithelial cells from the ectoderm of the CAM can be observed to proliferate and migrate into the hydrogels forming mutual fusional boundaries between the scaffolds and CAM tissues, which suggested the good biocompatibilities and bioactivities of these hydrogels mediating cell behaviors. Moreover, it should be particularly noted that new CAM tissue has grown into the peptide scaffold hydrogel of RAD/KLT. In the middle of the CAM stroma, blood vessels could be easily identified (marked by a black arrow in Fig. 6C2.) Matrigel was used as a positive control for evaluating angiogenesis in this study, in which clear CAM tissue invasion was noted with many scattered capillaries because of its abundance of angiogenic growth factors.

In the presence of VEGF within the peptide hydrogels, the representative histological sections (H&E staining) of the CAM with the different scaffolds are presented in Fig. 7. With the addition of VEGF, the peptide hydrogels RADA16-I, RAD/PRG, and RAD/KLT were all significantly invaded by hyperplastic CAM tissue with abundant capillary vessels, which was similar to results for collagen gel and Matrigel. No obvious differences were identified among these implants.

Discussion

Designing and screening ideal tissue-engineered scaffolds that promote endothelial cell migration, sprouting *in vitro* and capillary invasion *in vivo* has been the focus of angiogenesis. A class of designer peptide nanofiber scaffolds has been reported as a unique biological material in the application of angiogenesis.[20,25–28] In this study, we selected two functionalized peptides motifs including 2-unit RGD binding sequence PRG and VEGF-mimicking peptide KLT by directly extending the carboxyl termini of the self-assembling peptide RADA16-I to obtain the new functionalized peptide scaffolds. The functionalized peptide motifs have been reported to promote HUVEC proliferation and tubulogenesis in three-dimensional cell culture. Here, the endothelial cell migration and sprouting effected by the two peptides motifs were studied *in vitro* with dextran-coated microcarrier beads and their *in vivo* angiogenic activities were evaluated with the CAM model.

According to the 3D migration bead assay, we could see that the self-assembling peptide hydrogels provided appropriate synthetic cell microenvironments for extrinsic endothelial cell migration, which is the prerequisite of angiogenesis. Although all the peptide scaffolds showed positive effects on cell migration, the two functionalized peptide (RAD/PRG and RAD/KLT) scaffolds presented much higher bioactivities inducing HUVEC migration than the RADA16-I scaffold. The boundary-sandwiched cell migrations assay presented in our previous report also confirms the result.[20] The prominent differences among these peptide scaffolds are the functional motifs. It could therefore be concluded that the functional motifs KLT and PRG drive EC migration as the haptotaxis stimuli.[29,30]

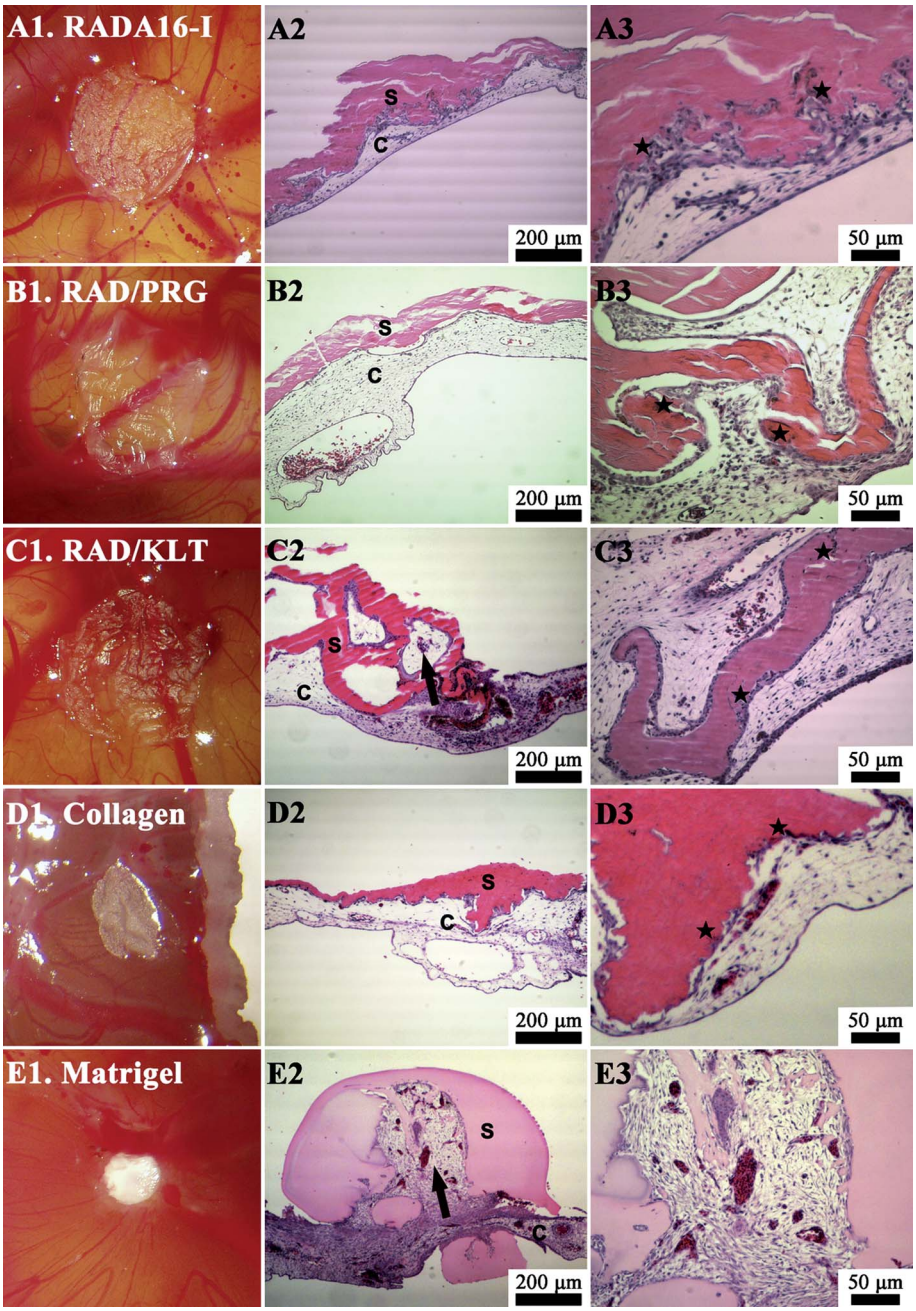

Fig. 6 Gross morphology and H&E staining of CAM with different scaffold hydrogels at day 4 after implantation. S: implanted hydrogels; C: the CAM. Black arrows indicate new capillary vessels. ★ indicates that epithelial cells from the ectoderm of CAM proliferate and migrate into the implanted hydrogels.

Endothelial cells sprouting from the parent vessel is the first and critical step in angiogenesis. Microcarrier beads have been extensively used for *in vitro* sprouts study.[23] In most *in vitro* angiogenesis models, endothelial cells sprout from the parent vessel, undergo morphological differentiation and reorganize into an extensive network of capillary-like structures in both

Table 2 Effect of functionalized peptide scaffold hydrogels on blood vessel density in CAM assay without VEGF

Scaffolds	RADA16-I	RAD/PRG	RAD/KLT
Blood vessel density (%)[a]	22.24 ± 1.12	34.55 ± 3.52[b]	49.81 ± 2.25[b]

[a] Data are presented as mean ± SD; $n = 10$. [b] $p < 0.01$ *vs.* RADA16-I, t-test.

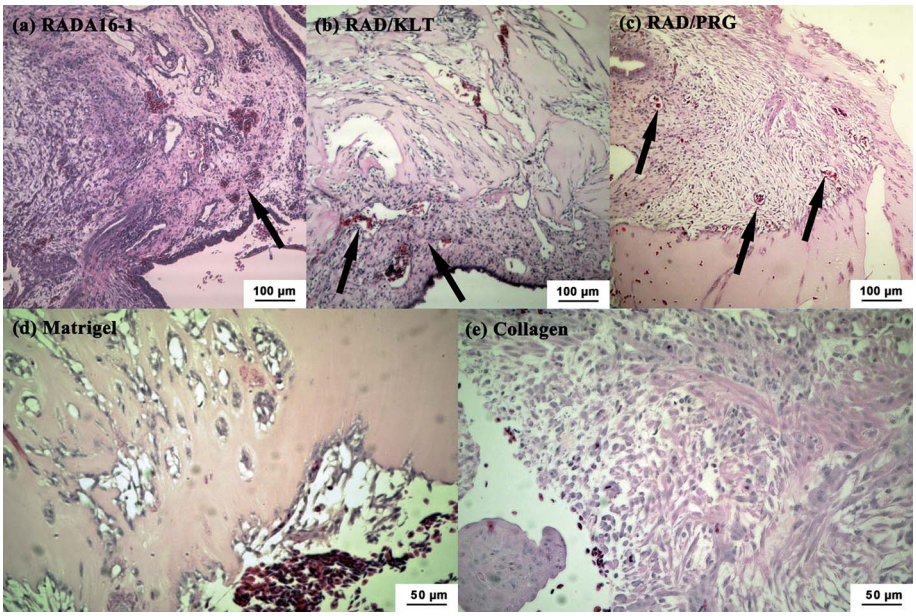

Fig. 7 H&E staining of CAM with VEGF in the peptide scaffold hydrogels at day 4 after implantation. Black arrows indicate new capillary vessels.

short-term and long term cultures depending on matrix and culture conditions.[31] Matsumoto *et al.*[32] have examined the effects of various growth factors on ECs sprouting in fibrin gel. VEGF only could promote cell migration from the dextran beads into the fibrin gel without sprouting. A combination of VEGF and HGF enhanced the number and length of sprouts in 3D culture. In our current studies, HUVECs could undergo sprouting from beads into the peptide scaffold hydrogels within one day in the present of VEGF only. Then ECs sprouting developed quickly and formed typical cord-like structures and branches with long processes especially in RAD/PRG and RAD/KLT gels, which is more evident than cell sprouting in collagen gel. According to the 3D migration and sprouting bead assays, it can be seen that the RAD/PRG and RAD/KLT play a vital role for stimulating EC migration, angiogenic sprouting and capillary lumen formation. In the absence of VEGF, the ECs underwent migration, while in the presence of VEGF, the ECs began sprouting, which is different from the results of Matsumoto's study. Although growth factors are quite indispensable for endothelial cell sprouting, these morphological differences among the hydrogels indicated that the functional motifs PRG and KLT might have promising effects on increasing the responsivity of endothelial cells to VEGF for sprouting.

VEGF/receptors and integrin $\alpha_v\beta_3$ are thought to be the most common protein systems involved in angiogenesis.[33,34] The VEGF mimicking sequence of KLT may mainly serve a similar function to VEGF that is bound to and activates the VEGF receptors, thus activating the VEGF-dependent proliferative pathway and inducing EC migration and sprouting.[35] Integrin $\alpha_v\beta_3$ could activate one or more intracellular signaling pathways necessary to cell survival, proliferation, differentiation, and migration after interaction with specific ECM ligands.[36] As RGD is the most relevant and investigated amino sequence that interacts with integrin $\alpha_v\beta_3$,[37] it is believed that PRG could activate "outside-in" and "inside-out" signaling through interaction with integrin $\alpha_v\beta_3$, thus contributing towards EC migration and sprouting.[38] In addition, ECs reside in the 3D environment, where the functional motifs on the nanofiber scaffolds surround the whole cell body in all dimensions and the extracellular matrix receptors on the cell membranes can bind to the functional ligands appended to the peptide scaffolds, receiving much more stimuli for migration and sprouting.

A CAM assay was carried out to assess the efficiency of various peptide scaffolds in inducing capillary invasion *in vivo*. The peptide scaffolds showed satisfactory biocompatibility with CAM tissue without severe inflammatory response. Among these three peptide scaffolds, RAD/KLT presents much better *in vivo* angiogenic activity inducing CAM tissue invasion and new capillary vessel formation within the scaffold in the absence of VEGF. With the addition of VEGF, more newly formed vessel lumen could be seen in all peptide scaffolds, which is similar to that observed for Matrigel. It is known that Matrigel contains many undefined growth factors that stimulate stroma cell invasion and capillary-like structure formation rapidly. The self-assembling peptide gels in combination with a low dose of VEGF have almost same effect as Matrigel in inducing angiogenesis. At the same time, the simple and definite compositions in the peptide hydrogel make it a novel and ideal class of tissue engineered scaffold with angiogenic ability for diverse applications in tissue engineering and tissue regeneration.

Perspective

Two functionalized self-assembling peptide scaffold hydrogels RAD/PRG and RAD/KLT were designed and evaluated specifically for angiogenesis in this study. The two functional motifs PRG and KLT significantly improved the bioactivities of self-assembling peptide RADA16-I and provided ideal synthetic microenvironments for endothelial cell migration, sprouting from microcarrier beads and capillary system invasion *in vivo* using a chick embryo CAM assay. At the same time, the

functional motifs might have promising effects on the responsivity of endothelial cells to VEGF for angiogenesis.

Acknowledgements

This work is in part supported by the National Natural Science Foundation of China (50803031, 50830102), the 863 Program (2011AA030105), Fok Ying Tung Education Foundation (122019), and Olympus Corporation.

References

1 Z. Y. Zhang, W. D. Ito, U. Hopfner, B. Bohmert, M. Kremer, A. K. Reckhenrich, Y. Harder, N. Lund, C. Kruse, H. G. Machens and J. T. Egana, *Biomaterials*, 2011, **32**, 4109–4117.
2 E. J. Suuronen, L. Muzakare, C. J. Doillon, V. Kapila, F. Li, M. Ruel and M. Griffith, *Int. J. Artif. Organs*, 2006, **29**, 1148–1157.
3 A. Wenger, A. Stahl, H. Weber, G. Finkenzeller, H. G. Augustin, G. B. Stark and U. Kneser, *Tissue Eng.*, 2004, **10**, 1536–1547.
4 D. J. Mooney and A. G. Mikos, *Sci. Am.*, 1999, **280**, 60–65.
5 C. K. Colton, *Cell Transplant.*, 1995, **4**, 415–436.
6 P. Carmeliet, *Nat. Med.*, 2000, **6**, 389–395.
7 W. Risau, *Nature*, 1997, **386**, 671–674.
8 X. Feng, M. Shaker, R. Clark and M. Tonnesen, *EJC Suppl.*, 2010, **8**, 90–91.
9 H. S. Yang, S. H. Bhang, J. W. Hwang, D. I. Kim and B. S. Kim, *Tissue Eng. A*, 2010, **16**, 2113–2119.
10 E. Ruvinov, J. Leor and S. Cohen, *Biomaterials*, 2010, **31**, 4573–4582.
11 C. P. Khoo, K. Micklem and S. M. Watt, *Tissue Eng., Part C*, 2011, **17**, 895–906.
12 J. G. Meingassner, M. Pillinger, H. Fahrngruber, E. Kowalsky and A. Stuetz, *J. Invest. Dermatol.*, 2011, **131**, S30–S30.
13 S. Endres, B. Hiebl, J. Hagele, C. Beltzer, R. Fuhrmann, V. Jager, M. Almeida, E. Costa, C. Santos, H. Traupe, E. M. Jung, L. Prantl, F. Jung, A. Wilke and R. P. Franke, *Clin. Hemorheol. Micro.*, 2011, **48**, 29–40.
14 C. K. Perng, Y. J. Wang, C. H. Tsi and H. Ma, *J. Surg. Res.*, 2011, **168**, 9–15.
15 Q. F. He, Y. N. Zhao, B. Chen, Z. F. Xiao, J. Zhang, L. Chen, W. Chen, F. L. Deng and J. W. Dai, *Acta Biomater.*, 2011, **7**, 1084–1093.
16 R. J. Lee, M. L. Springer, W. E. Blanco-Bose, R. Shaw, P. C. Ursell and H. M. Blau, *Circulation*, 2000, **102**, 898–901.
17 F. Gelain, A. Horii and S. Zhang, *Macromol. Biosci.*, 2007, **7**, 544–551.
18 A. Horii, X. Wang, F. Gelain and S. Zhang, *PLoS One*, 2007, **2**, e190.
19 D. Diana, B. Ziaco, G. Colombo, G. Scarabelli, A. Romanelli, C. Pedone, R. Fattorusso and L. D. D'Andrea, *Chem.–Eur. J.*, 2008, **14**, 4164–4166.
20 X. M. Wang, A. Horii and S. G. Zhang, *Soft Matter*, 2008, **4**, 2388–2395.
21 T. I. Valdes, D. Kreutzer and F. Moussy, *J. Biomed. Mater. Res.*, 2002, **62**, 273–282.
22 P. Nowak-Sliwinska, J. R. van Beijnum, M. van Berkel, H. van den Bergh and A. W. Griffioen, *Angiogenesis*, 2010, **13**, 281–292.
23 M. N. Nakatsu, R. C. A. Sainson, J. N. Aoto, K. L. Taylor, M. Aitkenhead, S. Perez-del-Pulgar, P. M. Carpenter and C. C. W. Hughes, *Microvasc. Res.*, 2003, **66**, 102–112.
24 M. Nguyen, Y. Shing and J. Folkman, *Microvasc. Res.*, 1994, **47**, 31–40.
25 A. Fedorova, K. Zobel, H. S. Gill, A. Ogasawara, J. E. Flores, J. N. Tinianow, A. N. Vanderbilt, P. Wu, Y. G. Meng, S. P. Williams, C. Wiesmann, J. Murray, J. Marik and K. Deshayes, *Chem. Biol.*, 2011, **18**, 839–845.
26 A. Adini, P. Erba, D. P. Orgill and R. J. D'Amato, *Wound Repair Regen.*, 2011, **19**, A8–A8.
27 Y. L. Song, Y. X. Li and Q. X. Zheng, *J. Wuhan Univ. Technol., Mater. Sci. Ed.*, 2010, **25**, 803–806.
28 A. Raiter, C. Weiss, Z. Bechor, I. Ben-Dor, A. Battler, B. Kaplan and B. Hardy, *J. Vasc. Res.*, 2010, **47**, 399–411.
29 V. Nehls, R. Herrmann and M. Huhnken, *Histochem. Cell Biol.*, 1998, **109**, 319–329.
30 R. L. Klemke, S. Cai, A. L. Giannini, P. J. Gallagher, P. de Lanerolle and D. A. Cheresh, *J. Cell Biol.*, 1997, **137**, 481–492.
31 B. Vailhe, D. Vittet and J. J. Feige, *Lab. Invest.*, 2001, **81**, 439–452.
32 T. Matsumoto, Y. C. Yung, C. Fischbach, H. J. Kong, R. Nakaoka and D. Mooney, *Tissue Eng.*, 2007, **13**, 207–217.
33 L. D. D'Andrea, A. Del Gatto, C. Pedone and E. Benedetti, *Chem. Biol. Drug Des.*, 2006, **67**, 115–126.
34 P. C. Brooks, R. A. Clark and D. A. Cheresh, *Science*, 1994, **264**, 569–571.
35 L. D. D'Andrea, G. Iaccarino, R. Fattorusso, D. Sorriento, C. Carannante, D. Capasso, B. Trimarco and C. Pedone, *Proc. Natl. Acad. Sci. U. S. A.*, 2005, **102**, 14215–14220.
36 D. D. Schlaepfer, C. R. Hauck and D. J. Sieg, *Prog. Biophys. Mol. Biol.*, 1999, **71**, 435–478.
37 A. van der Flier and A. Sonnenberg, *Cell Tissue Res.*, 2001, **305**, 285–298.
38 C. M. Longhurst and L. K. Jennings, *Cell. Mol. Life Sci.*, 1998, **54**, 514–526.